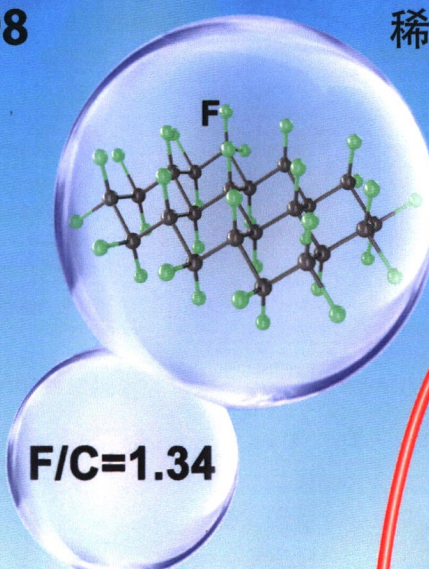


RARE METALS

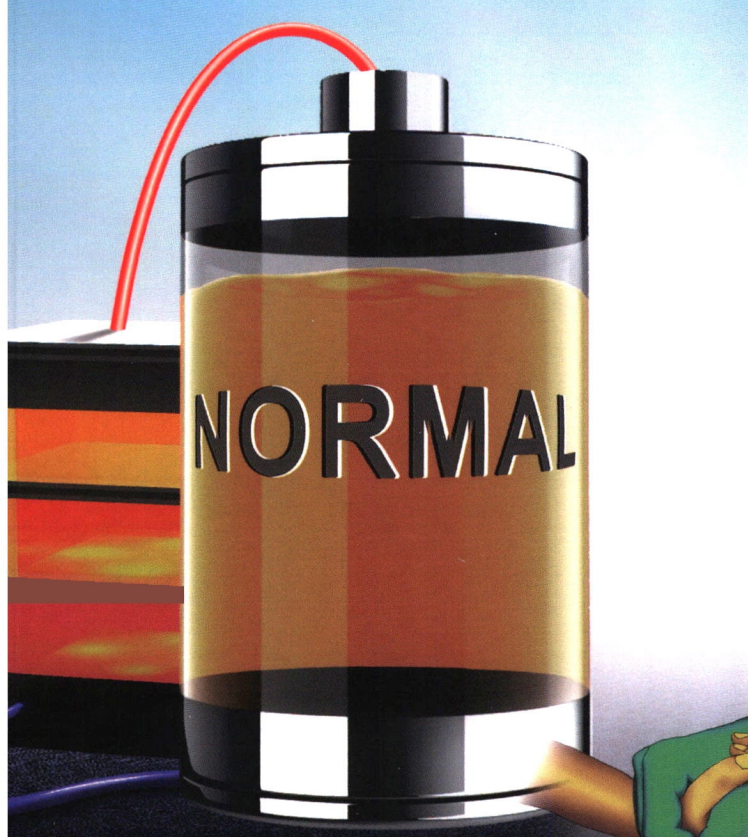
www.springer.com/journal/12598

稀有金属 (英文版)



Q K 2 1 3 1 8 5 7

F/C=1.34



RARE METALS (Monthly)

Volume 40 · Number 7 · July 2021

REVIEW

Recent progress in organic hole-transporting materials with 4-anisylamino-based end caps for efficient perovskite solar cells

X.-P. Xu · S.-Y. Li · Y. Li · Q. Peng **1669**

ORIGINAL ARTICLES

Cross-linkable fullerene interfacial contacts for enhancing humidity stability of inverted perovskite solar cells

M.-W. An · Z. Xing · B.-S. Wu · F.-F. Xie · S.-Y. Zheng · L.-L. Deng · X. Wang · B.-W. Chen · D.-Q. Yun · S.-Y. Xie · R.-B. Huang · L.-S. Zheng **1691**

Machine learning (ML)-assisted optimization doping of KI in MAPbI₃ solar cells

S. Jiang · C.-C. Wu · F. Li · Y.-Q. Zhang · Z.-H. Zhang · Q.-H. Zhang · Z.-J. Chen · B. Qu · L.-X. Xiao · M.-L. Jiang **1698**

Fluorinated graphite nanosheets for ultrahigh-capacity lithium primary batteries

X.-X. Yang · G.-J. Zhang · B.-S. Bai · Y. Li · Y.-X. Li · Y. Yang · X. Jian · X.-W. Wang **1708**

TiO₂-coated LiNi_{0.9}Co_{0.08}Al_{0.02}O₂ cathode materials with enhanced cycle performance for Li-ion batteries

W.-W. Li · X.-J. Zhang · J.-J. Si · J. Yang · X.-Y. Sun **1719**

Plasmonic photo-assisted electrochemical sensor for detection of trace lead ions based on Au anchored on two-dimensional g-C₃N₄/graphene nanosheets

J.-Y. Hu · Z. Li · C.-Y. Zhai · J.-F. Wang · L.-X. Zeng · M.-S. Zhu **1727**

Regulation of morphology and visible light-driven photocatalysis of WO₃ nanostructures by changing pH

Y.-S. Fan · X.-L. Xi · Y.-S. Liu · Z.-R. Nie · L.-Y. Zhao · Q.-H. Zhang **1738**

Photocatalytic properties of CaTi₂O₅ via a facile additive-free aqueous strategy with different pH values

W.-X. Dong · Q.-F. Bao · X.-Y. Gu · H.-J. Shen · P.-Y. Liu **1746**

La-enhanced Ni nanoparticles highly dispersed on SiC for low-temperature CO methanation performance

J.-W. Li · Q. Song · J.-B. Li · S.-C. Yang · Y.-S. Gao · Q. Wang · F. Yu **1753**

Enhanced positive humidity sensitive behavior of p-reduced graphene oxide decorated with n-WS₂ nanoparticles

Z.-H. Duan · Q.-N. Zhao · C.-Z. Li · S. Wang · Y.-D. Jiang · Y.-J. Zhang · B.-H. Liu · H.-L. Tai **1762**

Synthesis and NH₃/TMA sensing properties of CuFe₂O₄ hollow microspheres at low working temperature

K.-D. Wu · J.-Y. Xu · M. Debliquy · C. Zhang **1768**

Glycine-nitrate combustion engineering of neodymium cobaltite nanocrystals

E.A. Tugova · O.N. Karpov **1778**

Cerium–yttrium binary oxide microflower: synthesis, characterization and catalytic dehydration property

C. Pan · B.-H. Huang · C. Fan · X.-Y. Li · P.-G. Su · A.-Q. Zheng · Y. Sun **1785**

Synthesis and formation mechanism of nanocrystalline ZrB₂–Al₂O₃ composite powders via an amorphous precursor

S.-L. Song · Y.-L. Fan · R. Li · Y.-H. Lin · Q. Zhen **1801**

Pressure control as an effective method to modulate aggregative growth of nanoparticles

J. Xu · Y. Shu · Q. Xia · Y.-L. Guo · G.-J. Zhou · W.-C. Zhan **1808**

Self-propagating synthesis joining of C_r/Al composites and TC4 alloy using AgCu filler with Ni–Al–Zr interlayer

L. Shen · Z.-R. Li · G.-J. Feng · S.-Y. Zhang · Z. Zhou · P. He **1817**

Microstructure and properties of Al₂O₃–ZrO₂–TiO₂ composite coatings prepared by plasma spraying

P.-Y. Gao · Y.-D. Ma · W.-W. Sun · Y. Yang · C. Zhang · Y.-H. Cui · Y.-W. Wang · Y.-C. Dong **1825**

Post-deposition-annealed lanthanum-doped cerium oxide thin films: structural and electrical properties

V.N. Barhate · K.S. Agrawal · V.S. Patil · A.M. Mahajan **1835**

Tribological properties of plasma-sprayed nickel alloy matrix self-lubricating coating at elevated temperatures

W.-S. Li · Y. Sun · W. Hu · S.-Y. Zhu · H.-M. Zhai · J. Yang · X.-J. Fan · W.-M. Liu **1844**

- The tetragonal-like distortion of Fe–Ga alloys interstitial doped with Cu**
X. Zhao · X. Tian · Z.-Q. Yao · L.-J. Zhao · R. Wang · J. Yan **1851**
- Spontaneous positive exchange bias effect in SrFeO_{3-x}/SrCoO_{3-x} epitaxial bilayer**
T.-C. Su · J. Zhang · W. Zhang · Y.-Y. Wang · H.-H. Ji · X.-J. Wang · G.-W. Zhou · Z.-Y. Quan · X.-H. Xu **1858**
- Microstructural evolution and restoration of creep property for a damaged K403 alloy after rejuvenation heat treatments**
L. Wang · X.-G. Yang · H.-Y. Qi · D.-Q. Shi · S.-L. Li **1865**
- A new insight into rapid oxidation of alloy 925 contaminated by oxide powder**
H. Jiang · J.-X. Dong · M.-C. Zhang · J.-Y. Li **1872**
- Microstructure and mechanical properties of TC4 joints brazed with Ti–Zr–Cu–Sn amorphous filler alloy**
H.-H. Zhang · Z.-D. Cui · S.-L. Zhu · S.-W. Guo · X.-J. Yang · A. Inoue **1881**
- Enhanced strength and electrical conductivity of Al–0.3Ce alloy simultaneously with Ti(C,N) nanoparticle addition**
W.-P. Li · Y.-L. Zhang · J. Mao **1890**
- Microstructures and mechanical properties of a cast Al–Cu–Li alloy during heat treatment procedure**
S.-W. Duan · K. Matsuda · T. Wang · Y. Zou **1897**
- Transformation behavior of precipitates during artificial aging at 170 °C in Al–Mg–Si–Cu alloys with and without Zn addition**
S. Zhu · Z.-H. Li · L.-Z. Yan · X.-W. Li · S.-H. Huang · H.-W. Yan · Y.-A. Zhang · B.-Q. Xiong **1907**
- Chip morphology and cutting temperature of ADC12 aluminum alloy during high-speed milling**
X.-X. Meng · Y.-X. Lin **1915**
- Microstructure and corrosion properties of Mg–0.5Zn–0.2Ca–0.2Ce alloy with different processing conditions**
C. Zhang · L. Wu · G.-S. Huang · G.-G. Wang · B. Jiang · F.-S. Pan **1924**
- Microstructural development of vanadium–nickel crystalline alloy membranes**
P. Jiang · X.-B. Shi · B.-L. Sun · H.-C. Wang · M. Doland · G.-S. Song **1932**

- Oxidation behavior of multi-component Ta–W–Al–Ti alloy at 1173 K**
J.-X. Li · Y.-H. Chen · Z.-J. Bai · B.-J. Zhao · L. Jiang · L.-E. Wu **1940**
- Hot pressing sintering process and sintering mechanism of W–La₂O₃–Y₂O₃–ZrO₂**
B.-G. Fu · J.-C. Yang · Z.-K. Gao · Z.-R. Nie **1949**
- Dual-property blue and red emission carbon dots for Fe(III) ions detection and cellular imaging**
Y.-L. Xu · R.-X. Mo · C.-Y. Qi · Z. Ren · X.-Z. Jia · Z.-G. Kan · C.-L. Li · F. Wang **1957**
- Development of sandwich joining piece to fabricate segmented half-Heusler/skutterudite thermoelectric joints**
W.-A. Wang · X.-Y. Li · Y.-F. Xing · M. Gu · L.-H. Fang · Y.-F. Bao · J.-H. Fan **1966**
- Using highly concentrated chloride solutions to leach valuable metals from cathode-active materials in spent lithium-ion batteries**
A.-F. Yi · Z.-W. Zhu · Y.-H. Liu · J. Zhang · H. Su · T. Qi **1971**
- A novel approach to extract Nb, Y and Ce from a niobium-bearing ore of low grade by roasting KHSO₄–H₂SO₄ system**
W.-C. Gao · J.-K. Wen · B. Wu · H. Shang · X. Liu **1979**
- Equilibrium and mechanism studies of gold(I) extraction from alkaline aurocyanide solution by using fluorine-free ionic liquids**
Y.-T. Wang · M. Liu · N. Tang · S.-J. Li · Y. Sun · S.-X. Wang · X.-J. Yang **1987**

Cover Picture

X.-X. Yang et al. Fluorinated graphite nanosheets for ultrahigh-capacity lithium primary batteries

Further articles can be found at link.springer.com

Instructions for Authors for *Rare Met.* are available at www.springer.com/12598

RARE METALS (Monthly)

Volume 40 • Number 7 • July 2021

Cover story

(Xiao-Xia Yang, Guan-Jun Zhang, Bao-Sheng Bai, Yu Li, Yi-Xiao Li, Yong Yang, Xian Jian, Xi-Wen Wang*, pp. 1708–1718)

Fluorinated graphite nanosheets for ultrahigh-capacity lithium primary batteries

Lithium fluorocarbon (Li/CF_x) battery is the battery system with the highest specific energy in solid electrode chemical power supply. The F/C limit of conventional fluorocarbons is 1, and the theoretical specific capacity is $865 \text{ mAh} \cdot \text{g}^{-1}$. Because the energy of the material is difficult to be fully utilized in the practical battery, the specific energy of the battery is usually lower than $700 \text{ Wh} \cdot \text{kg}^{-1}$. At this concern, Wang et al. carried out innovative research on the preparation of fluorocarbon materials and electrodes, breaking through the F/C and specific capacity limits of existing fluorocarbon materials, and providing a new strategy for the realization of ultra-high specific energy lithium galvanic battery. By adjusting the temperature, the edge defects and $-\text{CF}_2$, $-\text{CF}_3$ perfluorinated functional group active sites are introduced into graphite nanosheets (NSs) in the form of covalent/ semi-covalent/ semi-ionic bonds, which broke the restriction of fluoro-carbon ratio to achieve ultra-thin microstructure with high performances. Using the ultra-high specific capacity CF_x NSs, combined with the "dual function" electrolyte that both conduct lithium ions and participate in the lithium synthesis reaction, and the lightweight battery structure design, a 24-Ah soft-packed lithium fluorocarbon primary battery with specific energy up to $1116 \text{ Wh} \cdot \text{kg}^{-1}$ was developed, which is the highest level reported in the relevant field at present.

Edited and Published by Youke Publishing Co., Ltd.
(No. 2, Xinjiekouwei Str., 100088 Beijing, China)

Tel.: +86 10 82241917; Fax: +86 10 82240869

Email: raremetals@grinm.com

Administrator: China Association for Science and Technology

Sponsor: The Nonferrous Metals Society of China
GRINM Group Co., Ltd.

Printer: Beijing Shengpinfengshang Technology Development Co., Ltd.,
Beijing, China

ISSN 1001-0521



9 771001 052213

07>

Price: RMB 300